Radar/Sonar Multitarget Tracking *

Marcelo G. S. Bruno and José M. F. Moura
Depart. Elect. and Comp. Eng., Carnegie Mellon University, Pittsburgh, PA, 15213
ph: (412)268-6341; fax: (412)268-3890; email:moura@ece.cmu.edu

Abstract: *This paper examines optimal joint detection and tracking of multiple targets that move randomly in spatially uncorrelated and correlated Gaussian and non-Gaussian (heavy tail) clutter. We develop an integrated detector/tracker and illustrate its performance with synthetic data.*

1 Introduction

The problem we consider in this paper is detection and tracking of multiple targets moving in cluttered environments. Given the sensor finite resolution, at each instant n, possible targets are either absent or centered in a given site on a finite discrete grid that represents the different resolution cells of the sensor. The sensor measurements are contaminated by clutter that accounts for false returns representing spurious reflectors and for measurement noise. Real targets move randomly on the finite sensor grid according to a known stochastic model.

The traditional approach to this problem decouples the detection and tracking tasks [1]: a predetection stage is followed by a data association algorithm that associates each possible validated measurement to a linearized tracking filter. By contrast, we integrate detection and tracking into the same framework. We apply nonlinear stochastic filtering to design the optimal multitarget joint detector/tracker. The resulting detector/tracker is a recursive Bayesian algorithm that incorporates the target, clutter, and motion models. Both spatially correlated Gaussian clutter and non-Gaussian clutter with heavy-tail statistics are considered. Further details on the implementation of the algorithm are found in [2].

2 The Model

We assume that, at each sensor scan, there may be at most M targets present in the surveillance space. Each target that is present is a rigid body with translational motion belonging to one of M possible classes characterized by their known, deterministic and time-invariant signature parameters and by the known dimensions of their noise-free image. We restrict our discussion to the situation where, at each sensor scan, there is only one possible target from each class. We do not exclude however the possibility of two or more classes being represented by the same signature parameters. For simplicity, we consider in this paper 1D surveillance spaces.

Sensor

The sensor scans a bounded 1D region. Given the sensor's finite resolution, this interval is discretized by a uniform finite discrete lattice

$$\mathcal{L} = \{l: 1 \leq l \leq L\} \tag{1}$$

where L is the number of resolution cells and l is an integer.

We introduce the vector

$$\mathbf{Z}_n = \left[z_n^1 \ \ldots \ z_n^M\right]^T \tag{2}$$

which collects the positions of the centroids of the M possible targets in the sensor image at instant n. In order to account for the situations when targets move in and out of the sensor range and in order to account for the possibility of absence of target, we define each random variable z_n^p on an *extended lattice*, [2],

$$\tilde{\mathcal{L}}_p = \{l: -l_s^p + 1 \leq l \leq L + l_i^p + 1\} \tag{3}$$

where $(l_i^p + l_s^p + 1)$ is the maximum length of the 1D noise free image of a class p target and $z_n^p = L + l_i^p + 1$ means that the class p target is absent at instant n.

Targets

Assuming real observations,the noise free image of a class p extended target, $1 \leq p \leq M$, is modeled as a mapping

$$\begin{aligned} \mathbf{t}_n^p: \ \tilde{\mathcal{L}}_p &\mapsto \Re^L \\ z_n^p &\to \mathbf{f}_p(z_n^p) \end{aligned} \tag{4}$$

*This work was supported by ONR grant no. N0014-97-0040. The first author was partially supported by CNPq-Brazil

0-7803-5045-6/98/$10.00 ©1998 IEEE

where

$$\mathbf{f}_p(z_n^p) = \sum_{k=-l_i^p}^{l_s^p} a_k^p \mathbf{e}_{z_n^p+k} \qquad z_n^p \in \overline{\mathcal{L}}_p \tag{5}$$

$$\mathbf{f}_p(z_n^p) = \mathbf{0}_L \qquad z_n^p = L + l_i^p + 1 \,. \tag{6}$$

In the previous model, $\mathbf{e}_l$, $1 \leq l \leq L$ is a vector whose entries are all zero, except for the lth entry which is one. If $l < 1$ or $l > L$, $\mathbf{e}_l$ is defined as the identically zero vector. The coefficients $\{a_k^p\}$ are the signature parameters of the class p target and $\overline{\mathcal{L}}_p = \{-l_s^p + 1 \leq l \leq L + l_i^p\}$ is the set of all possible positions of the centroid of a class p target such that at least one pixel of the target still lies on the sensor image.

A particular case of the generic extended target model is the pointwise target model, for which the target dimensions l_i and l_s are set to zero, meaning that the target is represented by only one single pixel in the sensor image.

Motion Model

The motion dynamics of a class p target in the corresponding extended lattice $\tilde{\mathcal{L}}_p$ is specified by a transition probability matrix $\mathbf{T}_p$ whose general element $T_p(k,j)$ is

$$T_p(k,j) \doteq \text{Prob}(z_n^p = k - l_s^p \mid z_{n-1}^p = j - l_s^p) \tag{7}$$

where $1 \leq k, j \leq L + l_i^p + l_s^p + 1$.

Observations

The observations at the nth sensor scan are

$$\mathbf{y}_n = \mathbf{f}_1(z_n^1) + \mathbf{f}_2(z_n^2) + \ldots + \mathbf{f}_M(z_n^M) + \mathbf{v}_n \tag{8}$$

where $\mathbf{v}_n$ is the background clutter and $f_p(z_n^p)$ is the appropriate model for a class p target (pointwise or extended). The observations model in (8) accounts for the possibility of superposition of target signatures or *merging target images.*

Clutter Models

We consider in this paper three models for the background clutter $\mathbf{v}_n$: spatially white Gaussian, spatially correlated Gaussian, and spatially white non-Gaussian clutter.

- **Gaussian clutter:** under the assumption of Gaussianity, the clutter vector $\mathbf{v}_n$ at each sensor scan has probability density function (pdf), $p(\mathbf{v}_n) = N(\mathbf{0}, \mathbf{R})$, where $\mathbf{R}$ is the clutter spatial covariance. We distinguish two cases:

  1. White Gaussian clutter: $\mathbf{R} = \sigma_u^2 \mathbf{I}$.
  2. Correlated Gauss-Markov clutter:

$$\sigma_u^2 \mathbf{R}^{-1} = \mathbf{I} - \sum_{p=1}^{m} [\alpha_p (\mathbf{K}_1^p + \mathbf{K}_2^p)] \,. \tag{9}$$

In (9), $\mathbf{I}$ is the identity matrix, and $\mathbf{K}_1$ and $\mathbf{K}_2$ are respectively the backward and forward shift matrix operators [2]. The clutter model corresponding to the inverse covariance in (9) can be interpreted as the output of the noncausal spatial finite difference equation [2]

$$v_n(i) = \sum_{p=1}^{m} \alpha_p [v_n(i-p) + v_n(i+p)] + u_n(i) \tag{10}$$

where $1 \leq i \leq L$ and $u_n(i)$ is a white Gaussian driving noise with covariance $\mathbf{\Sigma}_u = \sigma_u^2 \mathbf{I}$. The model in (9) assumes that *zero boundary conditions* are specified for the finite difference equation in (10).

- **Non-Gaussian clutter:** When dealing with non-Gaussian clutter, we assume in this paper that the sensor measures, for each resolution cell, the in-phase and quadrature returns of clutter and targets. The recorded clutter measurements at instant n correspond then to a sampling of the returned clutter complex envelope and are given by the even-sized vector

$$\mathbf{v}_n = [v_{c_n}^1 \, v_{s_n}^1 \, \ldots \, v_{c_n}^L \, v_{s_n}^L] \tag{11}$$

where L is the number of resolution cells. We assume that the double-sized vector $\mathbf{v}_n$ has a joint pdf with *non-Gaussian* statistics such that the sequence of random variables

$$e_k = \sqrt{(v_{c_n}^k)^2 + (v_{s_n}^k)^2} \quad 1 \leq k \leq L \tag{12}$$

is identically distributed with a probability density function different from a Rayleigh distribution. In this paper, we consider the K-envelope model for e_k. The K-pdf, which has been proposed as a model for sea clutter [4], is given by

$$p_E(e) = \frac{b^{\nu+1} e^{\nu}}{2^{\nu-1}\Gamma(\nu)} K_{\nu-1}(be) \qquad e \geq 0 \tag{13}$$

where ν is a shape parameter, $\Gamma(.)$ is the Eulerian function, $K_{\nu-1}(.)$ is a modified Bessel function of the second kind and b is related to average power σ^2 by $b^2 = \frac{2\nu}{\sigma^2}$.

We simulate samples of K-envelope clutter using segments of statistically independent spherically random vectors (SIRVS) with apropriate statistics. Details of the simulation are provided in [3].

3 Multitarget Detector/Tracker

Statement of the Problem

We assume that at each time instant an unknown number of targets ranging from zero to M may be present. The targets that are present belong to distinct classes (i.e., in the context of this model, have different signatures). Given the observations $\mathbf{y}_0^n$ from instant 0 up to instant n, we want, at each instant n, to perform three tasks: (1) determine how many targets are present/absent (detection); (2) assign the detected targets to a given class (data association); (3) estimate the positions of the detected targets in the lattice(tracking).

Optimal Bayesian Detector/Tracker

To accomplish these 3 tasks in an optimal Bayesian sense, it suffices to compute the joint posterior probability $P(\mathbf{Z}_n \mid \mathbf{y}_0^n)$ at each instant n. The formal solution is divided in 3 steps.

Filtering Step

From Bayes' law,

$$P(\mathbf{Z}_n \mid \mathbf{y}_0^n) = C_n p(\mathbf{y}_n \mid \mathbf{Z}_n) P(\mathbf{Z}_n \mid \mathbf{y}_0^{n-1}) \quad (14)$$

where C_n is a normalization constant.

Prediction Step

From the total probability theorem

$$P(\mathbf{Z}_n \mid \mathbf{y}_0^{n-1}) = \sum_{z_{n-1}^1} \cdots \sum_{z_{n-1}^M} P(z_n^1 \mid z_{n-1}^1) \cdots P(z_n^M \mid z_{n-1}^M) P(\mathbf{Z}_{n-1} \mid \mathbf{y}_0^{n-1}) \ . \quad (15)$$

Equation (15) assumes that the statistical models describing the motion of each target are independent.

Detection/Tracking

We now detail the minimum probability of error detector and the optimal MAP tracker for M targets.

1. Given $P(\mathbf{Z}_n \mid \mathbf{y}_0^n)$, compute the posterior probabilities of the detection hypothesis H_j, $0 \leq j \leq 2^M - 1$. The minimum probability of error detector decides that hypothesis H_i is true if $\forall j \neq i, 0 \leq i, j \leq 2^M - 1$,

$$P(H_i \mid \mathbf{y}_0^n) > P(H_j \mid \mathbf{y}_0^n) \ . \quad (16)$$

2. Let hypothesis H_0 correspond to the situation where all M targets are assumed present at instant n. If hypothesis H_i, $1 \leq i \leq 2^M - 1$, is declared true, introduce the conditional probability tensor $\mathbf{\Pi}_{n|n}^i$ defined as

$$\mathbf{\Pi}_{n|n}^i(\mathbf{Z}_n) = P(\mathbf{Z}_n \mid H_i, \mathbf{y}_0^n) = \frac{P(\mathbf{Z}_n, H_i \mid \mathbf{y}_0^n)}{P(H_i \mid \mathbf{y}_0^n)} \ . \quad (17)$$

The MAP Bayes tracker looks for the maximum of $\mathbf{\Pi}_{n|n}^i$ to estimate the positions of targets that are assumed present under hypothesis H_i.

4 Simulation Examples: Gaussian Clutter

We present in this section illustrative examples of joint detection and tracking of 2 targets in a 1D grid. We show initially examples with Gaussian background clutter. The examples include both pointwise and extended targets with white and spatially correlated Gaussian clutter. In section 5, we consider non-Gaussian clutter.

Pointwise Targets

Correlated Gaussian Clutter

We consider first an example where we detect and track 2 pointwise targets in spatially correlated Gaussian clutter. The targets are assumed to belong to two classes, respectively class 1 and class 2, which are characterized by their deterministic signatures. Class 1 targets have a deterministic signature $a_1 = 1$ while class 2 targets have a deterministic signature $a_2 = 0.8$. The targets move in the lattice with average drifts $d_1 = 2$ for class 1 targets, and $d_2 = 4$ for class 2 targets, and have a fluctuation probability of one cell of $p = q = 0.4$ around their average displacement. The background clutter is a first order noncausal Gauss-Markov sequence (GMRseq) with $\alpha_1 = 0.25$. The peak signal-to-noise ratio is PSNR_1 =14 dB for class 1 targets and PSNR_2 =12 dB for class 2 targets.

The lattice is assumed to have $L = 64$ resolution cells and the simulation extends over 70 time scans. At each scan, either two targets (one from each class) are present, or only one target is present, or none of the targets is present in the lattice. Once a target disappears from the sensor range, a new target from the same class can appear at any cell with a probability of $p_a = 0.3$.

The detection/tracking results for class 1 targets are shown in figure 1(a). The results for class 2 targets are shown in figure 1(b). The correct track is shown in solid line whereas the estimated track is marked by the symbol '+'. The actual absence of a target during a given scan is represented by the symbol 'o' plotted over the the corresponding time index on the horizontal axis. Likewise, an estimated absence of target is marked by the symbol '+' plotted on the horizontal axis.

The detection statistics for class 1 and class 2 targets for the levels of PSNR in figure 1 were obtained through Monte Carlo simulations using 10,000 sensor scans. The results are shown in table 1 for two different numbers of resolution cells: $L = 64$ and $L = 100$.

Extended Targets

Next, we present an example where we

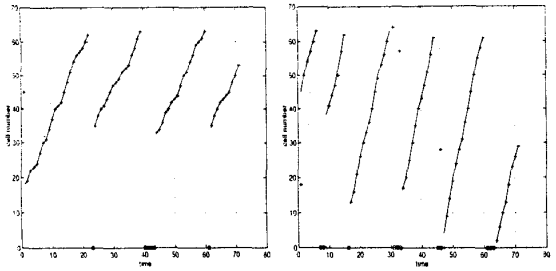

(a) (b)

Figure 1: (a) Tracking of class 1 targets in first order GMRseq clutter, PSNR_1=14dB, (b) Tracking of class 2 targets in first order GMRseq, PSNR_2=12 dB

Detection Statistics	$L = 64$	$L = 100$
P_{d_1}	0.9926	0.9946
P_{f_1}	0.0393	0.0242
P_{d_2}	0.9665	0.9798
P_{f_2}	0.0434	0.0499

Table 1: Detection statistics with correlated Gaussian clutter, PSNR_1 = 14 dB, PSNR_2 = 12 dB

track/detect two extended targets in a 1D finite grid, against a white Gaussian background clutter. Both class 1 and class 2 targets extend over 9 resolution cells with $l_i = r_i = r_s = l_s = 4$, but have different (deterministic) amplitude distributions. Specifically, class 1 targets have a rectangular-shaped signature, whereas class 2 targets have a triangular-shaped signature.

In a given sensor scan, either two targets (one class 1, the other class 2) are present, or just one target (either class 1 or 2) is present, or no target is present. In this simulation, we assume that, in a given scan with two targets present, the corresponding sensor returns may be either apart from each other, as shown in figure 2, or superimposed in the scan image, as shown in figure 3.

The targets have translational motion with the position of the targets centroids in the 1D grid described by known first order discrete Markov chains with deterministic drifts $d_1 = 2$ and $d_2 = 4$ for class 1 and class 2 targets, respectively. Like in our simulation with pointwise targets, once a target belonging to a given class disappears from the sensor range, another target of the same class can appear randomly at any resolution cell with a probability $p_a = 0.3$. The simulation was conducted for 100 time steps (100 simulated sensor scans), assuming 100 resolution cells per scan.

Figures 4 (a) and (b) show the centroid detection/tracking results assuming PSNR equal to 3 dB. Despite some small deviations in the estimated position of the centroids and an increased propensity to misses for class 2 targets, the simulation indicates that the overall performance of the detector/tracker does not deteriorate significantly in face of high noise power, even during sensor scans where the signatures of the two targets are merged as in figure 3.

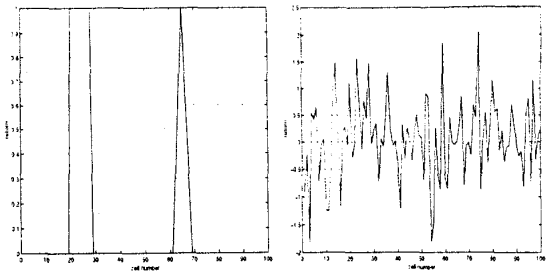

(a) (b)

Figure 2: (a)Noise-free sensor scan with two targets. (b) Observed (noisy) sensor scan, PSNR=3 dB

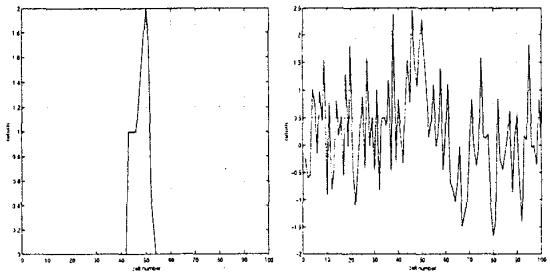

(a) (b)

Figure 3: (a)Noise-free sensor scan with superimposed targets. (b) Observed sensor scan, PSNR=3 dB

5 Simulation Examples: Non-Gaussian Clutter

In this section, we present an example where we detect/track two targets against non-Gaussian background clutter with K-distributed envelope statistics. As mentioned before, in the case of non-Gaussian clutter, we treat the observations as complex vectors or, equivalently, real vectors with double length, that collect the sensor measurements of the in-phase and quadrature returns from the targets and the clutter. For simplicity, the targets are assumed to be pointwise targets with a deterministic amplitude signature in the in-phase component.

We denote the ith element, $i \in \mathcal{L}$, of the complex

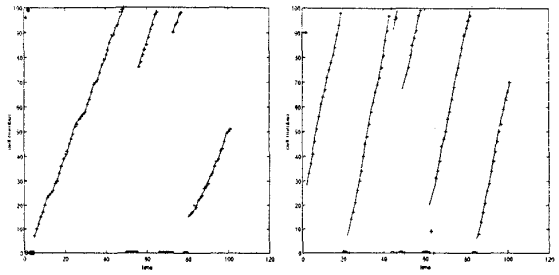

(a) (b)

Figure 4: (a) Centroid tracking for class 1 targets. (b) Centroid tracking for class 2 targets, PSNR = 3 dB

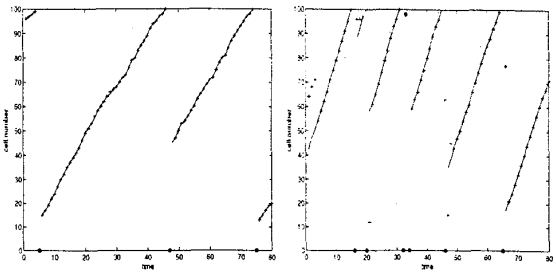

(a) (b)

Figure 5: (a) Tracking of class 1 targets in K-envelope clutter, $PSNR_1$=10 dB, (b) Tracking of class 2 targets in K-envelope clutter, $PSNR_2$=8.5 dB

image $\mathbf{f}^1(z_n^1)$ of a class 1 target located at z_n^1 during the nth sensor scan by $f^1(z_n^1)_i$. The target signature is then specified as follows:

$$\begin{aligned} f^1(z_n^1)_i &= [a^1\ 0] \qquad z_n^1 = i \\ f^1(z_n^1)_i &= [0\ 0] \qquad z_n^1 \neq i\ . \end{aligned} \tag{18}$$

Similarly, the ith element, $i \in \mathcal{L}$, of the complex image $\mathbf{f}^2(z_n^2)$ of a class 2 target located at z_n^2 at instant n is given by

$$\begin{aligned} f^2(z_n^2)_i &= [a^2\ 0] \qquad z_n^2 = i \\ f^2(z_n^2)_i &= [0\ 0] \qquad z_n^2 \neq i\ . \end{aligned} \tag{19}$$

If z_n^1 or z_n^2 are equal to $L+1$, $\mathbf{f}(z_n^1)$ or $\mathbf{f}(z_n^2)$ are defined as an identically zero vector.

The sensor grid is assumed to have $L = 100$ resolution cells and the simulation is carried out over 80 sensor scans, each one corresponding to 200 returns (2 per cell). The peak signal-to-noise ratio per scan is $PSNR_1$ =10 dB for class 1 targets and $PSNR_2$ =8.5 dB for class 2 targets.

Figures 5(a) and 5(b) show the detection/tracking results for class 1 and class 2 targets respectively. As before, once a target of a given class disappears, there is a probability $p_a = 0.3$ of a target of the same class reentering the sensor grid at a random resolution cell.

Notice that, for class 2 targets (for which the PSNR is comparatively lower), the tracker seems to get initially confused as a new target appears in the sensor image. The confusion is eliminated, however, and a correct track is established as soon as new data is available and incorporated through the filtering step of the algorithm. For class 2 targets, we also notice an increased propensity to false alarms and misses.

6 Conclusion

In this paper, we presented an integrated framework for optimal joint detection/tracking of multiple targets that move randomly on a finite discrete grid. Both extended and pointwise targets with deterministic signatures were considered. Illustrative simulation examples using both white and correlated Gaussian background clutter, and non-Gaussian clutter with K envelope indicate good detection/tracking performance even in adverse noisy environments.

References

[1] Y. Bar-Shalom and X. Li.*Multitarget-Multisensor Tracking: Principles and Techniques.* YBS, Storrs, CT, 1995.

[2] M. G. S. Bruno. *Joint Detection and Tracking of Moving Targets in Clutter.* Ph.D. Thesis, ECE Department, Carnegie Mellon University, May 6, 1998.

[3] M. G. S. Bruno and J. M. F. Moura. *Optimal Detection and Tracking of Randomly Moving Targets in Clutter.* To be presented in the IEEE International Symposium on Telecommunications, São Paulo, Brazil, August 1998.

[4] C. J. Oliver. *Representation of Radar Sea Clutter.* IEE Proceedings, 135, Pt. F, 6, December 1988, pp. 497-500.